Towards improving the electroanalytical speciation analysis of indium

Elise Rotureau*[,1,2], Pepita Pla-Vilanova[3], Josep Galceran[3], Encarna Companys[3], José Paulo Pinheiro[1,2]

[1] CNRS, LIEC (Laboratoire Interdisciplinaire des Environnements Continentaux), UMR7360, Vandoeuvre-lès-Nancy F54501, France.

[2] Université de Lorraine, LIEC, UMR7360, Vandoeuvre-lès-Nancy F54501, France.

[3] Departament de Química, Universitat de Lleida and AGROTECNIO, Rovira Roure 191, 25198 Lleida, Catalonia, Spain

Keywords: indium, free metal, AGNES, SCP, electroanalytical techniques, speciation

ABSTRACT

The geochemical fate of indium in natural waters is still poorly understood, while recent studies have pointed out a growing input of this trivalent element in the environment as a result of its utilisation in the manufacturing of high-technology products. Reliable and easy-handling analytical tools for indium speciation analysis is, then, required. In this work, we report the possibility of measuring the total and free indium concentrations in solution using two complementary electroanalytical techniques, SCP (Stripping chronopotentiometry) and AGNES (Absence of Gradients and Nernstian Equilibrium Stripping) implemented with the TMF/RDE (Thin Mercury Film/Rotating Disk Electrode). Subnanomolar limits of detection were obtained for both techniques in the experimental conditions used in this work, e.g. 0.5 nM for SCP and 0.1nM for AGNES, and can be further improved consenting longer experiment times. We also verified that AGNES was able (i) to provide robust speciation data with the known In-oxalate systems and (ii) to elaborate indium binding isotherms in presence of humic acids extending over 4 decades of free indium concentrations.

The development of electroanalytical techniques for indium speciation opens up new routes for using indium as a potential tracer for biogeochemical processes of trivalent elements in aquifers, *e.g.* metal binding to colloidal phases, adsorption onto (bio)surfaces, etc.

1. Introduction

In the context of extensive expansion of low-carbon energy technologies, indium has been classified by the EU commission as a near-critical metal regarding the risk of supply chain bottlenecks [1]. The principal industrial application of indium worldwide is for producing indium oxide (In_2O_3) and indium tin oxide (ITO) to make electrically conducting transparent thin films, mainly used for liquid crystal displays and photovoltaic cells. The world's indium production has increased tenfold since the nineties [2]. Indium is almost exclusively obtained as a by-product in zinc smelters operating using sphalerite (a zinc sulphide ore mineral). Besides, the potential of indium recyclability is relatively limited [3]. It is now recognized that the steadily increased use of indium for technology applications is leading to a significant anthropogenic input in the biogeochemical cycle of indium [4]. While measured total amounts of indium in freshwaters are usually low *e.g.* ranging from 1 to 15 pM in Japanese rivers [5], more abundant concentrations are found in (i) groundwaters, with reported values of 81 nM and 0.18 μM in Canada [6] and in a polluted site in Taiwan [7], respectively, (ii) acid mine drainage waters, where the amount may reach up to 0.25 μM [8] (iii), soils with measured average values of 0.15 μmol kg^{-1} [9] and (iv) sediments, with measured values ranging from 0.13 to 0.87 μmol kg^{-1} [10].

In recent years, there is a growing interest in the environmental fate [6,9] and toxicity [11–13] of indium, but they remain mostly unknown [4]. The aqueous geochemistry of indium is very close to other trivalent ions such as gallium and scandium, elements that are all heavily influenced by hydrolysis reactions [14]. In aqueous solution, indium acts as a hard acid which preferentially interacts with ligands containing oxygen donor atoms, *e.g.* hydroxides, carboxylate and phenolate groups. As for other metal cations, the fate of indium will likely be controlled by its interaction with natural organic matter (NOM) and/or with the mineral surfaces, mostly clays or iron hydro-oxides [15]. Since the understanding of metal speciation is

considered as a key issue for evaluating the adverse effects of metallic contamination in natural ecosystems and especially in aquifers, and there are growing demands for on-site indium detection, robust and versatile techniques for laboratory set-up need to be urgently developed. To date, analytical determinations of indium in the environment are commonly performed using inductively coupled spectroscopy and atomic absorption spectroscopy preceded usually by a pre-concentration step [4]. Therefore, current efforts are made to conceive new techniques trying to minimize handling steps before the measurement of free or total indium concentrations in aqueous samples. Among them, ion selective electrodes have been successfully designed with organic solid-contact indium sensors reaching the detection threshold of 0.1 μM [16,17]. Electroanalytical sensors offer great opportunities to quantify the total indium amount at micromolar concentrations levels, using ex-situ plated antimony film [18–20] or bismuth film [21] electrodes. Another study reported the analytical performance of the adsorptive stripping electrochemical techniques (AdSV) in terms of linear ranges of calibration and limits of detection [22]. Because AdSV requires the addition of a complexing agent, further speciation analyses are more involved. Very recently, the technique Absence of Gradients and Nernstian Equilibrium Stripping (AGNES), commonly used for free ions quantification of trace metal elements [23–25], has been extended to indium analysis with a sensitivity below nanomolar concentrations [26]. This equilibrium technique provides new perspectives for acquiring thermodynamic information pertaining to indium binding properties with molecular or colloidal ligands. As detailed in this pioneering work, the methodology using mercury drop electrodes still necessitates some improvements regarding the measurement reproducibility and the rather long acquisition times which can exceed 30 min [26].

In this work, we report the possibility of measuring the total and the free indium concentrations using two complementary electroanalytical techniques. The first one is Stripping chronopotentiometry (SCP) [27] which is used to quantify the total indium amount in the

samples, after a preliminary acidification step. SCP is a stripping technique, thus presenting a very low detection limit, typically on the nanomolar level, and furthermore is not affected by the adsorption of organic ligands at the surface of the working electrode [28]. The second technique exploited in this work, AGNES [29] is employed for the direct determination of the free metal concentration, thus providing an estimation of the stability constants of the complexed metal species in solution.

This study explores the analytical indium sensing performance and robustness of these two techniques using a thin film mercury electrode (TMFE) deposited on a rotating disk electrode (RDE). The results demonstrate the added advantages of these two techniques *e.g.* their easy handling, high sensitivity (sub-nanomolar detection limits), good reproducibility and ability to perform indium speciation studies.

2. Material and methods

2.1.Reagents and solutions

All solutions were prepared with ultra-pure water (18.2 MΩ cm, Elga labwater). In(III) and Hg(II) solutions were obtained from dilution of a 1000 mg L^{-1} certified standard solution (Fluka). The ionic strength is set with sodium perchlorate ($NaClO_4$) (Fluka, >>98%), perchlorate acid ($HClO_4$) (Fluka) or sodium hydroxide (NaOH) (Merck suprapur) solutions were used to adjust the pH. Nitrogen (>99.999% pure) for the electrochemical experiments was purchased from Air Liquide. Ammonium acetate (NH_4Ac), ammonium thiocyanide (NH_4SCN) and hydrochloric acid (HCl) (all p.a. from Merck) were used to prepare the solution for the cleaning of the working electrode and re-dissolution of the mercury film. Oxalate solution was obtained from solid sodium oxalate ($Na_2C_2O_4.2H_2O$) from (Fluka, >99.5% pure). The humic substances were extracted following the IHSS procedure for soil organic matter [30] from peat in the Mogi river region of Ribeirão Preto, São Paulo State, Brazil. The elemental analysis

yielded C: 51.3%; H: 4.2% and N: 3.8% with an ash content of 0.6%, while potentiometric titrations showed carboxylic and phenolic groups of 3.2 and 3.0 mol kg^{-1} respectively, well within the usual values for a peat humic acid [31].

2.2.Apparatus

An Ecochemie Autolab type III potentiostat controlled by GPES 4.9 software (Ecochemie, The Netherlands) was used in conjunction with a Metrohm 663VA stand. Dri-ref-5 electrode from WPI (Sarasota, U.S.A.) and a glassy carbon electrode were used as reference and counter electrode, respectively. The working electrode was a thin mercury film (TMF) plated onto a rotating glassy carbon disk of 2 mm diameter (Metrohm) as detailed in section 2.3. The preparation of the rotating disk/thin mercury film electrode (TMF/RDE) was repeated daily for each set of experiments.

2.3.Working electrode preparation

The first step consists in polishing the electrode surface using alumina (Metrohm) slurry for 1 min, followed by a thorough washing with ultrapure water, then sonicating the electrode in ultrapure water during 1 min.

The second step consists in an electrochemical pre-treatment of 50 successive cyclic voltammograms between -0.8 and +0.8 V at 0.1 V s^{-1} in NH_4Ac 1 M /HCl 0.5 M solution [32].

The third step is the electrodeposition of the thin Hg film. So, the glassy carbon was immersed in a Hg(II) solution 0.12 to 0.24 mM (pH 1.9) and deposited using a potential of -1.3 V for a period of time ranging from 240 s to 420 s using a rotation rate of 1000 or 1500 rpm. The different conditions produce electrodes of different thicknesses, thus after each working day, the charge associated with the deposited Hg was determined to assess the state of the mercury film. This was carried out by electronic integration of the linear sweep stripping peak of Hg

with a scan rate v = 0.005 V s^{-1} in 5 mM of ammonium thiocyanide (pH 3.4) using a stripping range from -0.15 V to +0.4 V [25].

2.4.Experimental protocol

In the laboratory set-up, a disposable polystyrene cell is placed in a double-walled container connected to a refrigerated-heating circulator and the temperature of the solution is set to 25°C. The solution is initially purged using nitrogen for 15 min and afterwards a nitrogen blanket is always maintained above the sample solution.

SCP experimental parameters are as follows: (i) the deposition step is carried out at the specified deposition potential E_d in the limiting current region for a set time, t_d (between 45 and 180 s) using a rotation rate of 1000 rpm (ii) a stripping current, I_s of 3 µA, under non-rotating conditions, is applied until the potential reaches a value well past the reoxidation transition plateau, typically E_d=-0.700V.

AGNES measurements were performed following the hereafter detailed protocol. The metal deposition step at the Hg electrode was achieved by applying a potential E_d fixed for a suitable deposition time (t_d) using a rotation rate of 1000 rpm. The magnitude of the potential E_d is chosen in order to accumulate a sufficient amount of indium to be safely quantified, while establishing a situation without concentration gradients in the solution at the vicinity of the electrode surface and Nernstian equilibrium (more details in the section 3 of the supplementary material) within a reasonable time. The gain (or preconcentration factor) Y is the ratio between the concentrations of reduced and oxidised metal at equilibrium. The charge (Q) of the stripping stage (in the variant called AGNES-SCP [33]) was taken as response function. It has been shown that the measured stripping charge is proportional to the free metal concentration, which for indium reads:

$$Q = Y\,\eta_Q\,[In^{3+}] \qquad (1)\text{Nernst}$$

where [In^{3+}] is the free indium concentration and η_Q is a proportionality factor that (due to Faraday's law) can be computed from the mercury volume V_{Hg}, as

$$\eta_Q = 3\,F\,V_{Hg} \qquad (2)\text{Nernst}$$

where F is the Faraday constant.

The experimental protocol for calibration measurements, for both SCP and AGNES, consists of preparing a solution made up from 20 mL of 100 mM $NaClO_4$, 60 µL of 1M $HClO_4$ to fix the pH at 2.5, so as *ca.* 97.4% of indium is in free from, according to Visual MinteQ [34] using Biryuk's constants [35]. Then several additions of indium stock solution 10 µM and 100 µM are achieved to construct the calibration plots.

The determination of free indium in presence of oxalate was carried out for a total indium concentration of 0.6 µM at pH 3 with various sodium oxalate concentrations *i.e.* 10, 20, 40 and 100 µM and at pH 4 with sodium oxalate concentration of 10, 20 and 40 µM.

2.5.Quantification of free indium in humic acids suspensions by using AGNES

Batch suspensions of 5 mg L^{-1} purified humic acids stabilized in 100 mM $NaClO_4$ electrolyte were prepared. Indium concentration was fixed at values in the concentration range of 0.1 µM to 2.5 µM. Then, the pH was fixed at 3.75 by addition of $HClO_4$ and the solutions were equilibrated at least 24 h prior to the measurements. Before the determination of the free indium concentration, a calibration plot was performed using the AGNES parameters previously mentioned. The batches were disposed in the electrochemical cell and AGNES measurement was repeated three times to determine the free indium concentration.

3. Results and Discussion

3.1 Total metal determination

The determination of the total concentration of indium by electrochemistry in natural samples needs a previous acidification step to pH values equal or below 2.5 in order to destroy

complexes with organic matter or particles and to prevent the formation of indium hydroxides. This is best achieved using $HClO_4$, due to the absence of indium perchlorate complexes, which is not the case with nitrate, sulphate [36] or chlorates [14].

As mentioned in the introduction, environmental concentrations of indium in natural waters vary from extremely low values in surface waters (picomolar) to relatively high (sub-micromolar) values in polluted groundwater. In soils and sediments, the content per kg lies in a relatively large interval with an average value close to 150 nmol kg^{-1}. Thus, the target detection limit should be as low as possible to account for the surface waters concentrations, while being able at the same time to reach the relatively high concentration values to measure sediment and soil extracts.

The detection linearity range obtained with for a unique time deposition of 45 s is very large for indium element when using mercury electrodes. As observed in Figure S1 of the supplementary material (section 1), the linearity domain reaches upper concentrations of 30 μM. This high value stems from the extraordinary amalgamation of indium in mercury (up to 57% (w/w)), which is the highest of all metals [37].

Regarding the detection limit, the electroanalytical stripping techniques have the potential to reach extremely low values due to the pre-concentration in the deposition step. Observing the equations for SCP (section 2 in supplementary material), SCP key parameters are stripping current (I_s) and deposition time (t_d) in Eq. (S2.3) and electrode area (A) and thickness of the diffusion layer (δ) in Eq. (S2.4).

The detection limit in SCP is conditioned by the presence of dissolved oxygen, since it can reoxidise chemically the amalgamated metal. For the TMF/RDE case, this problem may be minimized using relatively large oxidising currents (I_s), thus competing with the chemical oxidation induced by the dissolved oxygen in solution. Our previous experience with performing SCP in TMF/RDE's showed that I_s larger than 10 μA tends to increase the noise in

the signal, so that a trade-off combination of an I_s on the order of 2-5 μA coupled with a reasonable nitrogen purge (usually 15 to 20 minutes) followed by blanketing the system with nitrogen provides the best results in terms of detection limit. Applying values of I_s lower than 1 μA demands longer purging times driving the method unsuitable for field conditions.

Regarding the electrode area, the commercial electrodes are normally circular with diameters spanning over 2 and 5 mm. This size is constrained by the three electrodes cell configuration used in voltammetry that demands a counter electrode (significantly) larger than the working electrode. Also increasing the electrode area might increase the instrumental noise meaning that the detection limit gain may be marginal.

The third parameter is the thickness of the diffusion layer (δ) which is dependent on cell geometry and hydrodynamic conditions. In the case of the RDE, increasing the rotation speed will provide better detection limits, however this might impact negatively on the stability of the mercury film. We have observed that the RDE rotation speed should not exceed 1500 rpm to obtain durable electrodes.

So, for the parameters discussed above, several constrains define their values leaving only the deposition time (t_d) as a relatively free parameter to obtain better detection limits for total indium determination in acidic media.

Figure 1 shows the calibration plots obtained for deposition times 45, 90 and 180 s with TMF/RDE using a rotation speed of 1000 rpm and E_d=-0.700V, at pH 2.3 in 100 mM $NaClO_4$. The calculated detection limits from the standard deviation of residuals ($LOD=3s_y/m$ with s_y the standard deviation of the blank response and m the slope of the calibration curve) of the calibration curve for the different deposition times are 21 nM for 45 s, 13 nM for 90 s and 0.5 nM for 180 s. According to Eq. (S2.3) of the supplementary material, whenever the oxygen current is negligible in front of I_s, the signal is the product of the deposition time and limiting current, which depends directly on the (total) metal concentration in solution (for a solution

with no complexation). Since the LOD is computed using the standard deviation of residuals and the slope of the calibration plot, it can be reasoned that if the signal is good enough, the standard deviation of residuals will be reasonably constant, hence the LOD will be inversely proportional to the slope of the calibration plot. This hypothesis seems to be well confirmed by the results presented in Figure 1, where a fourfold increase in deposition time (45 s to 180 s) produced a fourfold decrease in LOD (2 to 0.5 nM). Following this correlation, a LOD of 0.1 nM would require a fivefold increase in deposition time from 180 s to 900 s (15 min).

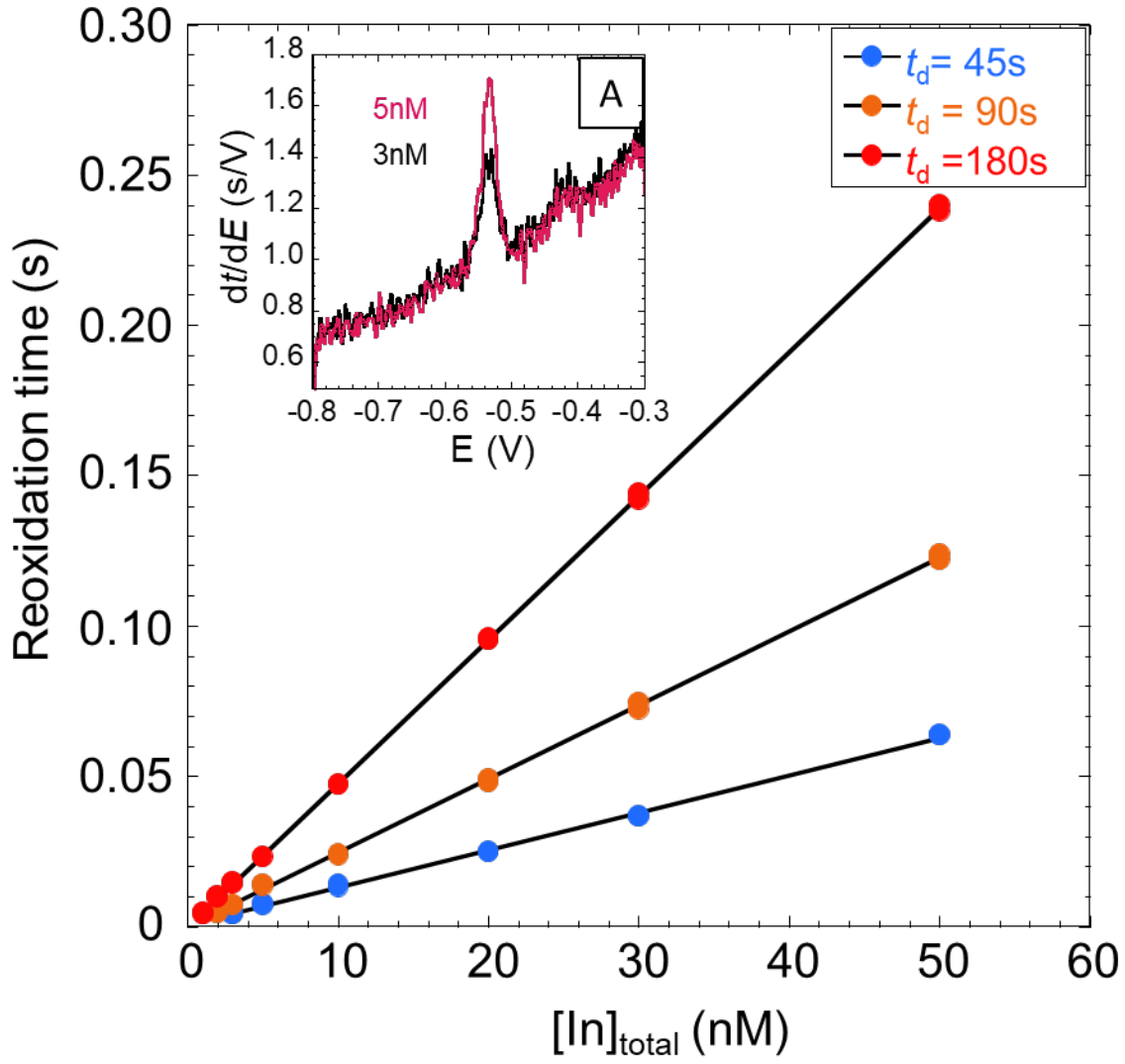

Figure 1: SCP calibrations for deposition times of 45 s (blue), 90 s (orange) and 180 s (red) at E_d=-0.700V, obtained with the TMF/RDE ~~of 3mm~~, rotation speed 1000 rpm, in 100 mM $NaClO_4$ medium, pH 2.3. Inset: SCP curves for indium concentration of 3 and 5 nM for the deposition time of 180 s showing the signal to noise ratio.

The inset of Figure 1 depicts two SCP curves for 3 and 5 nM indium giving some insight on the signal to noise ratio. We point out that the signal is the area under the peak and not the peak height.

3.2 Free metal determination

According to Tehrani *et al* [26], the free In^{3+} quantification can be performed using AGNES in a hanging drop mercury electrode (HMDE) which provides a good detection limit. However, they reported repeatability problems and a relatively long analysis time, typically 800 s. To overcome these limitations, we replaced the working HMDE by the TMF/RDE, exhibiting a larger surface to volume ratio, thereby potentially reducing the measurement time [38].

From a theoretical point of view, the detection limit for a free metal ion using AGNES depends on the gain (*i.e.* the deposition potential, Eq. (S3.1) of the section 3 of the supplementary material), implying that it effectively depends on the amount of time we are willing to wait until reaching equilibrium. Reasonability constrains these deposition times to less than one hour (a few experimental points per day), and practicality to times up to 10 minutes.

With this in mind, we tested AGNES with our TMF/RDE system by carrying out calibration plots for indium in $NaClO_4$ medium at pH 2.5, initially using deposition potentials roughly in the mid-point of the ancillary Scanning Stripping Chronopotentiometry wave [39] and sufficiently long deposition times to reach equilibrium.

A total of 51 calibrations plots were carried out at 10 mM, 30 mM and 100 mM $NaClO_4$ ionic strength. Repeatability of the calibrations was tested involving three different operators and three voltammetry stands.

Table S1 of section 4 in the supplementary material shows that the detection limits (LOD) determined using the standard deviation of residuals of the calibration plot range from a

minimum of 0.7 nM to a maximum 9.5 nM free indium, depending both on the gain used and the noise of the baseline.

The results obtained are repeatable and, during the experimental work, we only discarded one working day, thus demonstrating the robustness of this method. The detection limit obtained in experimental conditions is very satisfactory.

The advantage of AGNES is that, by using more negative deposition potentials, the gain (Y) increases, and in turn, the detection limits decreases, provided that a sufficiently long deposition time is applied to guarantee equilibrium.

Following Tehrani *et al* [26], the gain (Y_{calib}, associated to the applied potential E_{calib}) is not computed from any ancillary polarographic experiment, but, rather, from the calibration (based on Eq. (3)), once the proportionality factor η_Q is determined from the mercury volume using Eq. (2).

Figure 2 shows the calibration plots obtained in 100 mM $NaClO_4$ at pH 2.6 for different deposition potentials ranging from -0.5850 V to -0.5950 V, where it can be observed that the slope increases significantly corresponding to the calculated gains from 20500 to 58500.

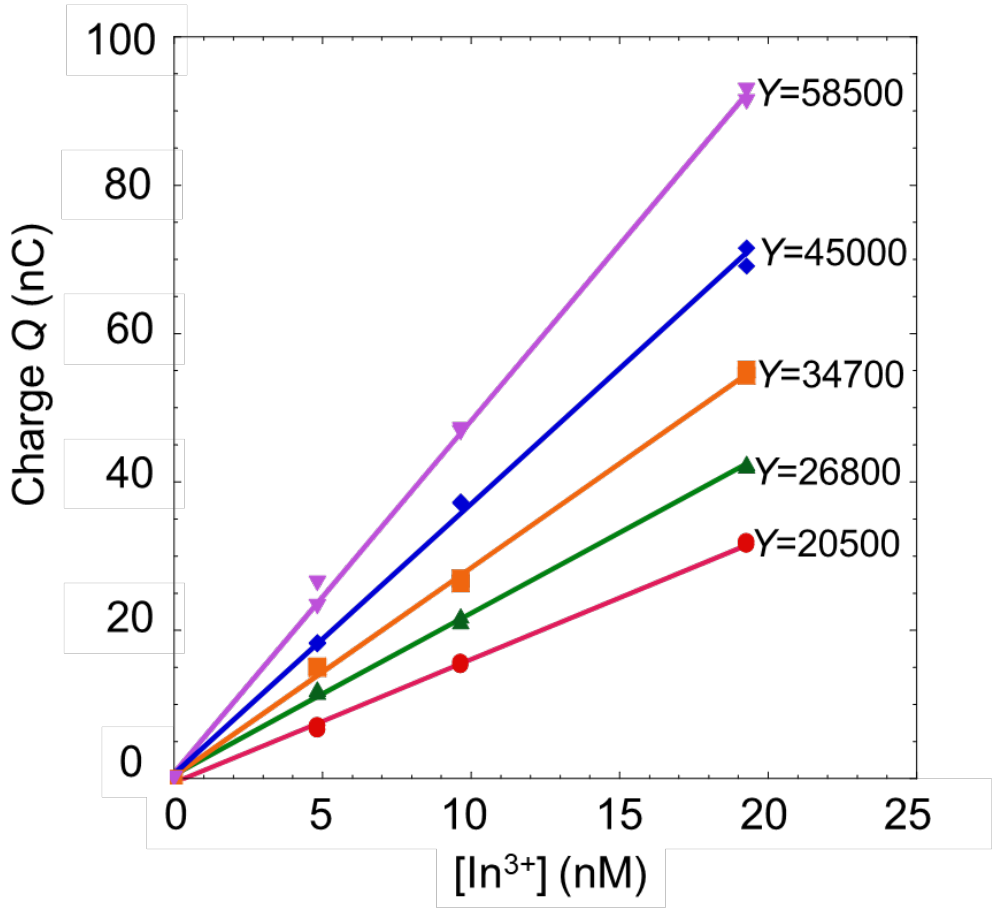

Figure 2: AGNES calibrations at pH 2.6 in 100 mM $NaClO_4$ medium, using different E_d: -0.5850 V, t_d=180 s (red dot), -0.5875 V, t_d=210 s (green triangle), E_{calib}= -0.5900 V, t_d=240 s (orange square), E_{calib}=-0.5925 V, t_d=330 s (blue diamond) and E_{calib}=-0.5950 V, t_d=390 s (purple triangle). Free indium concentration has been computed by Visual MinteQ [34] using Biryuk constant values [35]. The calculated gain (Y) for each calibration plot is reported.

In order to reach better detection limits, better gains from the calibrated ones might be necessary. This can be safely done as long as the measurement corresponds to the same calibration interval for Q and one checks that the equilibrium condition is attained for the pair deposition potential/deposition time. Deposition potentials (E_j) for new gains (Y_j) can be computed taking into account Nernst equation, given the expected linearity of the logarithm of the gain with the deposition potential:

$$\ln(Y_j/Y_{\text{calib}}) = -\left(\frac{3F}{RT}\left(E_j - E_{\text{calib}}\right)\right) \qquad \text{(3)Nernst}$$

To confirm that the equilibrium condition is attained, we performed a series of trajectories which consist in measuring the accumulated charge in the electrode upon the increase of the deposition times for given deposition potentials. Figure 3 shows the different trajectories obtained for 30 nM indium solution in 100 mM $NaClO_4$ at pH 2.6 obtained for several deposition potentials indicated in the figure caption. As depicted in Figure 3A, all trajectories asymptotically tend towards plateau values for sufficiently large deposition time, evidencing that the equilibrium state is reached after a suitable accumulation stage. The results clearly show that, for more negative deposition potentials, the equilibrium time is longer and the charge (or gain) is higher.

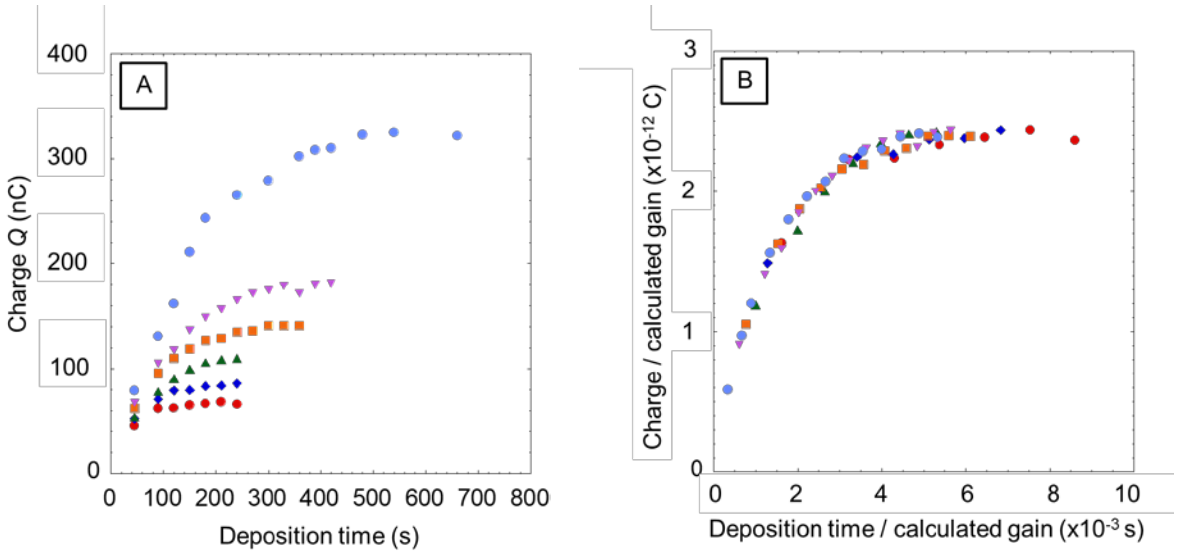

Figure 3: Experimental trajectories (A) obtained for deposition potentials of -0.5850 V (red dot), -0.5875 V (blue diamond), -0.5900 V (green triangle), -0.5925 V (orange square), -0.5950 V (purple triangle) and -0.6000 V (light blue circle) for 30 nM indium concentration in 100 mM $NaClO_4$, pH 2.6 and for a rotation speed of 1000 rpm, and normalized trajectories (B) by the calculated gain (Y) as a function of the deposition time over Y.

Figure 3B reports the trajectories normalized by the gain as determined from the calibration plots constructed for each deposition potential. This so-obtained master curve allows an estimation of the empirical relationship between the equilibrium deposition time and the gain. Thus, we obtain $t_d=5\times10^{-3}Y$ (s). The proportionality factor is significantly smaller than the value

of 10 obtained by Tehrani *et al* [26] using the HMDE, meaning that for a certain gain, the TMF/RDE will reach equilibrium 2000 times faster than the HMDE.

As shown in Figure 4, we validate the Nernstian behaviour of the electrochemical system by plotting the linear dependence of $\ln(Y_j/Y_{calib})$ vs. E_j-E_{calib} (Eq. (3)), according to the experimentally determined couple (E_{calib}; Y_{calib}).

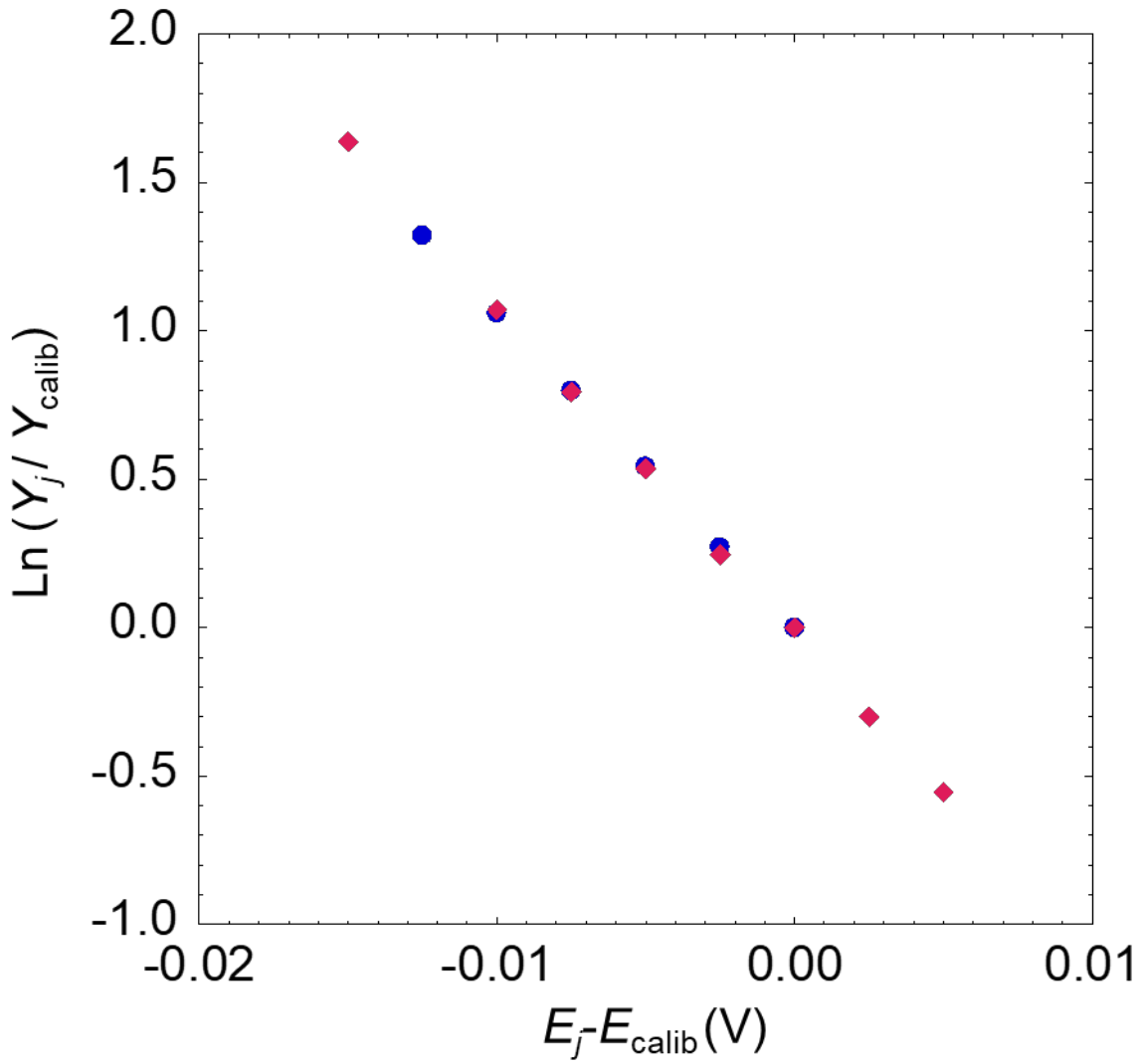

Figure 4: Dependence of $\mathrm{Ln}(Y_j/Y_{calib})$ according to Eq. (S3.4) for a solution of 30 nM indium in 100 mM $NaClO_4$ at pH 2.6, with rotation speed 1000 rpm. Different deposition potentials were employed (blue) -0.5825 V, -0.5850 V, -0.5875 V, -0.5900 V, -0.5925 V, -0.5950 V and (red) -0.5750 V, -0.5775 V, -0.5800 V, -0.5825 V, -0.5850 V, -0.5875 V, -0.5900 V and -0.5950 V.

This Nernstian behaviour is the key to one of the most striking AGNES feature which allows probing a very large range of detection limits, as depicted in Figure 3. The establishment of a

calibration at a certain concentration range (for instance from 10 to 300 nM of indium) provides the initial couple (E_{calib}; Y_{calib}). Then, it is possible to target a relevant gain (Y_j) using Eq. 3 derived from Nernst relationship, by applying the calculated E_j. This is particularly helpful in the construction of indium binding isotherms over a wide range of metal coverage of the reactive sites. We will address this feature in detail in the following section for the speciation of indium in presence of complexing ligands.

3.3 The hydrolysis of indium

As for most trivalent metal ions, indium speciation in an aqueous solution is heavily influenced by hydrolysis reactions. AGNES calibration is performed in acidic condition to warrant the predominance of the free form. Although it is expected that no complex species can interfere in the determination of free indium with AGNES, upon pH increase, electrochemically active species $In(OH)^{2+}$ can help in reaching equilibrium faster [40].

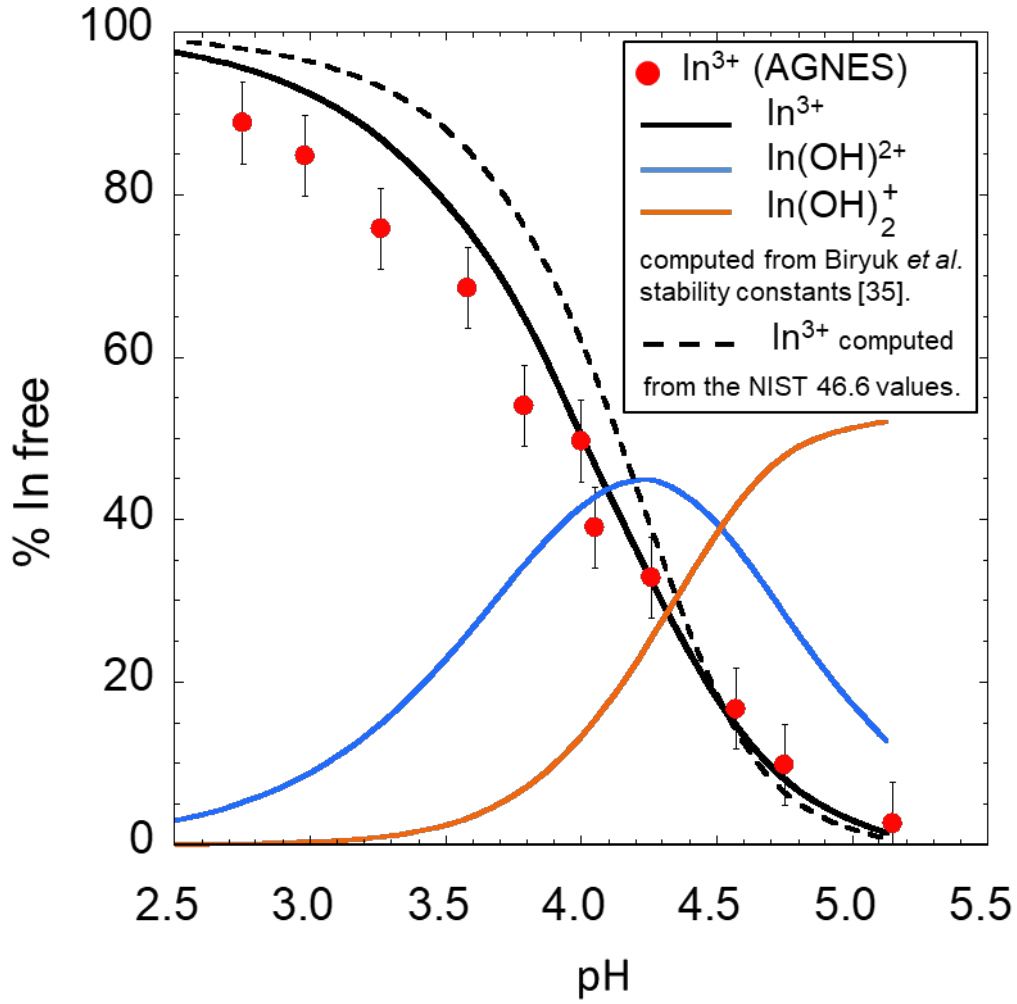

Figure 5: pH dependence of the percentage of free indium in 100 mM $NaClO_4$ experimentally determined by the AGNES technique and compared to the thermodynamic speciation of indium according to the stability constants in [14,35]. The total concentration of indium is 50 µM. The rotation speed is 1000rpm, E_d=-0.580V and t_d=120 s. Error bars are estimated from the relative uncertainties over three AGNES measurements.

So, we compared the experimental AGNES results with the thermodynamic speciation according to Biryuk *et al* [35] and the NIST 46.6 database in the pH range of 2.5 to 5.5. Figure 5 shows a slightly better agreement between the percentages of free ions as determined by AGNES with those computed by Visual MinteQ using the following values of hydrolysis of In^{3+} logK_1=-3.54, logK_2=-7.82 and logK_3=-12.98 from Biryuk *et al* [35] at infinite dilution. As expected from its principles, AGNES is measuring the free indium concentration without any special interference from a possible electroactive $In(OH)^{2+}$. Indeed, when we reach the

equilibrium by the end of the deposition stage of AGNES, In^{3+} is in equilibrium with In^0, and In^{3+} is in equilibrium with $In(OH)^{2+}$ (like in the bulk, if we have absence of gradients in the concentrations profiles), so $In(OH)^{2+}$ should also be in equilibrium with In^0. The only impact expected from $In(OH)^{2+}$ being more electroactive than In^{3+} is a contribution from $In(OH)^{2+}$ to the (transient) accumulation flux, so that the approach to the equilibrium should be faster, but the finally accumulated amount is not influenced by other complexes.

3.4 Speciation of indium with oxalate and humic acids

After establishing that the species measured by AGNES is indeed the free In^{3+}, it is fundamental to evaluate its performance in speciation studies.

Figure 6 shows that the results obtained in this study for In-oxalate binding are in reasonable agreement with previously published results, since they lie halfway between the ones reported by Pingarron *et al* [41] and the ones reported by Vasca *et al* [42]. In a previous work using AGNES in the HMDE Tehrani *et al* [26] using somewhat different experimental conditions observed values closer to the ones reported by Vasca *et al* [42]. We must warn that, because of a typing error, the total concentration of indium of 100 μmol L^{-1} was unduly reported as 5 μmol L^{-1} in the caption of figure 6 in [26].

We estimated the errors for our AGNES measurements using the 95% confidence interval obtained from the standard deviation of the 4 measurements multiplied by Student factor for binomial distributions ($t_{95,3}$=3.182). As expected, the errors are larger for the smaller values obtained at pH 4, since they are closer to the detection limit.

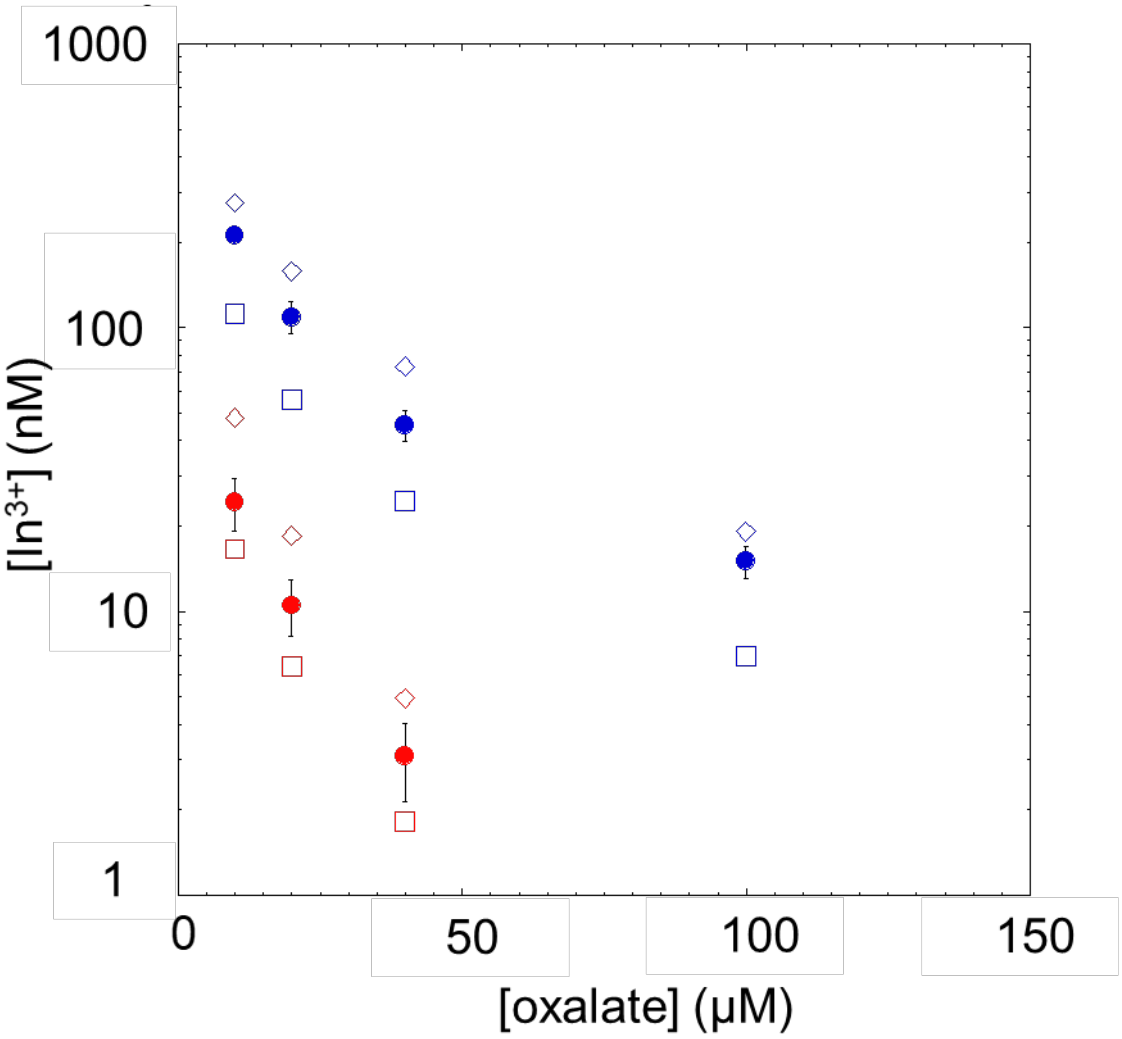

Figure 6: Free indium concentrations measured by AGNES in presence of increasing concentrations of oxalate in 100 mM $NaClO_4$ at pH 3 (blue circle) and pH 4 (red circle). Total indium concentration is 0.1 μM. The rotation speed is 1000 rpm. Computed values using Visual MinteQ with the stability constants determined by Pingarron *et al* [41] (open diamond) and Vasca *et al* [42] (open square).

One of our main interests in developing these methodologies is the ability to perform indium speciation directly in environmental samples. Since the interaction of indium with natural organic matter (NOM) is expected to be one of the key parameters, about which there is no information in the literature, we decided to test AGNES in presence of a well-characterised humic sample [31], as a representative colloidal phase in freshwaters.

Figure 7 depicts an indium titration of 5 mg L^{-1} of humic acid substance, at pH 3.75, 100 mM $NaClO_4$, *i.e.*, the free indium evolution as a function of the total indium concentration added.

The red points at very low indium concentration were obtained using the strategy of changing the deposition potential and computing the new gain using Eq. (3.3). In this particular case the calibration linked E_{calib} = –0.580V with Y_{calib} = 1.6×10^4 and the new gain for the experiment in presence of humic acids at E_d = –0.630V was Y = 3.3×10^6. In this way, four decades of free indium concentrations are probed by the AGNES technique with reasonable equilibrium times (less than 10 min). Thus, this methodology opens the way to the elaboration of indium binding isotherms over a wide range of metal coverage to humic acid particles. Moreover, we observe a reasonable repeatability amongst the different measurement (replicates) demonstrating the ability of AGNES to provide robust speciation data.

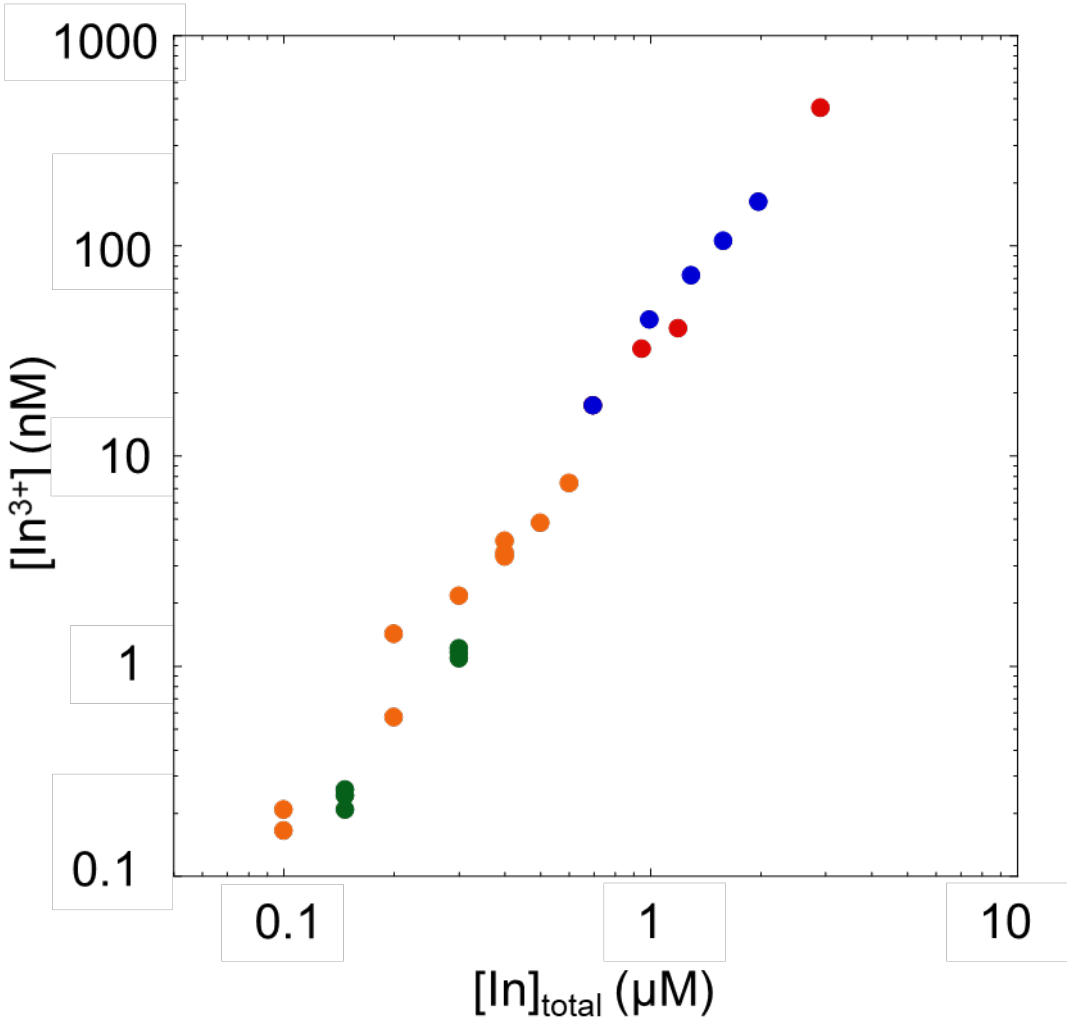

Figure 7: Free indium concentrations measured by AGNES in several suspensions of humic acids (5 mg L^{-1}) containing known total indium concentrations, at pH 3.75 and ionic strength of 100 mM $NaClO_4$.

The rotation speed is 1000 rpm. Each colour corresponds to replicates. Error bars estimated from the relative uncertainties over three AGNES measurements, are smaller than points.

Conclusions

In this work we investigated the ability of two electroanalytical techniques to measure low concentration of total (SCP) and free indium (AGNES). For the total concentration, at pH <2.3, we obtained an excellent detection limit of 0.5 nM for 180 s deposition time.

For the free metal determination using AGNES, we demonstrated the enormous saving in experimental time when using the TMF/RDE instead of the HMDE and confirmed the excellent performance of these electrodes in speciation studies, especially when determining extremely low free indium concentrations (down to 10^{-10} M). We also verified that AGNES was able to provide robust speciation data in experiments in presence of humic matter.

Due to the absence of trivalent cation complexation data with humic matter, it is our intention to pursue these studies with experiments at different pH values and different ionic strengths, followed by adequate complexation modelling, especially at higher pH values where the influence of indium hydrolysis will be noticeable. Such investigations will open new perspectives for using indium as a powerful tracer of geochemical processes of trivalent elements in terrestrial waters.

Acknowledgements

This work has been supported by the French National Research Agency through the national program “Investissements d’avenir” with the reference ANR-10-LABX-21-01 / LABEX RESSOURCES21. We thank the contribution of Jérémy Gloux, Paco Iglesias and Mirella Dammous from University of Lorraine in the preliminary experimental work. Funding from the Spanish Ministry of Economy, Industry and Competitiveness MINECO, project CTM2016-

78798 (EC, PPV, JG) is acknowledged. PPV thanks Generalitat de Catalunya for a doctoral FI-AGAUR fellowship.

Supplementary material

Section 1: Linearity range for In^{3+} in SCP with TMF/RDE.

Section 2: Stripping Chronopotentiometry (SCP) at the TMF/RDE.

Section 3: Fundamentals of AGNES.

Section 4: Calibration plots obtained with AGNES.

AUTHOR INFORMATION

Corresponding Author

*Email: elise.rotureau@univ-lorraine.fr

References

[1] European Commission, Critical Metals in the Path towards the Decarbonisation of the EU Energy Sector: Assessing Rare Metals as Supply-Chain Bottlenecks in Low-Carbon Energy Technologies, (2013). https://ec.europa.eu/jrc/en/publication/eur-scientific-and-technical-research-reports/critical-metals-path-towards-decarbonisation-eu-energy-sector-assessing-rare-metals-supply.

[2] U.S. Geological Survey, 2017, Mineral commodity summaries 2017, (2017). https://doi.org/10.3133/70180197.

[3] L. Ciacci, B.K. Reck, N.T. Nassar, T.E. Graedel, Lost by Design, Environ. Sci. Technol. 49 (2015) 9443–9451. doi:10.1021/es505515z.

[4] S.J.O. White, H.F. Hemond, The Anthrobiogeochemical Cycle of Indium: A Review of the Natural and Anthropogenic Cycling of Indium in the Environment, Crit. Rev. Environ. Sci. Technol. 42 (2012) 155–186. doi:10.1080/10643389.2010.498755.

[5] Y. Nozaki, D. Lerche, D.S. Alibo, M. Tsutsumi, Dissolved indium and rare earth elements in three Japanese rivers and Tokyo Bay: Evidence for anthropogenic Gd and In, Geochim. Cosmochim. Acta. 64 (2000) 3975–3982. doi:10.1016/S0016-7037(00)00472-5.

[6] A. Tessier, C. Gobeil, L. Laforte, Reaction rates, depositional history and sources of indium in sediments from Appalachian and Canadian Shield lakes, Geochim. Cosmochim. Acta. 137 (2014) 48–63. doi:10.1016/j.gca.2014.03.042.

[7] H.-W. Chen, Gallium, Indium, and Arsenic Pollution of Groundwater from a Semiconductor Manufacturing Area of Taiwan, Bull. Environ. Contam. Toxicol. 77 (2006) 289–296. doi:10.1007/s00128-006-1062-3.

[8] S.J.O. White, F.A. Hussain, H.F. Hemond, S.A. Sacco, J.P. Shine, R.L. Runkel, K. Walton-Day, B.A. Kimball, The precipitation of indium at elevated pH in a stream

influenced by acid mine drainage, Sci. Total Environ. 574 (2017) 1484–1491. doi:10.1016/j.scitotenv.2016.08.136.

[9] A. Ladenberger, A. Demetriades, C. Reimann, M. Birke, M. Sadeghi, J. Uhlback, M. Andersson, E. Jonsson, GEMAS: Indium in agricultural and grazing land soil of Europe - Its source and geochemical distribution patterns, J. Geochem. Explor. 154 (2015) 61–80. doi:10.1016/j.gexplo.2014.11.020.

[10] K. Folens, G. Du Laing, Dispersion and solubility of In, Tl, Ta and Nb in the aquatic environment and intertidal sediments of the Scheldt estuary (Flanders, Belgium), Chemosphere. 183 (2017) 401–409. doi:10.1016/j.chemosphere.2017.05.076.

[11] N.R. Brun, V. Christen, G. Furrer, K. Fent, Indium and Indium Tin Oxide Induce Endoplasmic Reticulum Stress and Oxidative Stress in Zebrafish (Danio rerio), Environ. Sci. Technol. 48 (2014) 11679–11687. doi:10.1021/es5034876.

[12] C. Zeng, A. Gonzalez-Alvarez, E. Orenstein, J.A. Field, F. Shadman, R. Sierra-Alvarez, Ecotoxicity assessment of ionic As(III), As(V), In(III) and Ga(III) species potentially released from novel III-V semiconductor materials, Ecotoxicol. Environ. Saf. 140 (2017) 30–36. doi:10.1016/j.ecoenv.2017.02.029.

[13] C.I. Olivares, J.A. Field, M. Simonich, R.L. Tanguay, R. Sierra-Alvarez, Arsenic (III, V), indium (III), and gallium (III) toxicity to zebrafish embryos using a high-throughput multi-endpoint in vivo developmental and behavioral assay, Chemosphere. 148 (2016) 361–368. doi:10.1016/j.chemosphere.2016.01.050.

[14] S.A. Wood, I.M. Samson, The aqueous geochemistry of gallium, germanium, indium and scandium, Ore Geol. Rev. 28 (2006) 57–102. doi:10.1016/j.oregeorev.2003.06.002.

[15] A. Tessier, C. Gobeil, L. Laforte, Reaction rates, depositional history and sources of indium in sediments from Appalachian and Canadian Shield lakes, Geochim. Cosmochim. Acta. 137 (2014) 48–63. doi:10.1016/j.gca.2014.03.042.

[16] V.K. Gupta, A.J. Hamdan, M.K. Pal, Comparative study on 2-amino-1,4-naphthoquinone derived ligands as indium (III) selective PVC-based sensors, Talanta. 82 (2010) 44–50. doi:10.1016/j.talanta.2010.03.055.

[17] M.N. Abbas, H.S. Amer, A Solid-Contact Indium(III) Sensor based on a Thiosulfinate Ionophore Derived from Omeprazole, Bull. Korean Chem. Soc. 34 (2013) 1153–1159. doi:10.5012/bkcs.2013.34.4.1153.

[18] C. Pérez-Ràfols, N. Serrano, J.M. Díaz-Cruz, C. Ariño, M. Esteban, Simultaneous determination of Tl(I) and In(III) using a voltammetric sensor array, Sens. Actuators B Chem. 245 (2017) 18–24. doi:10.1016/j.snb.2017.01.089.

[19] J. Zhang, Y. Shan, J. Ma, L. Xie, X. Du, Simultaneous Determination of Indium and Thallium Ions by Anodic Stripping Voltammetry Using Antimony Film Electrode, Sens. Lett. 7 (2009) 605–608. doi:10.1166/sl.2009.1117.

[20] H. Sopha, L. Baldrianova, E. Tesarova, S.B. Hocevar, I. Svancara, B. Ogorevc, K. Vytras, Insights into the simultaneous chronopotentiometric stripping measurement of indium(III), thallium(I) and zinc(II) in acidic medium at the in situ prepared antimony film carbon paste electrode, Electrochimica Acta. 55 (2010) 7929–7933. doi:10.1016/j.electacta.2009.12.089.

[21] I. Geca, M. Korolczuk, Sensitive Anodic Stripping Voltammetric Determination of Indium(III) Traces Following Double Deposition and Stripping Steps, J. Electrochem. Soc. 164 (2017) H183–H187. doi:10.1149/2.0581704jes.

[22] K.C. Honeychurch, Recent Developments in the Stripping Voltammetric Determination of Indium, World J. Anal. Chem. World J. Anal. Chem. 1 (2013) 8–13. doi:10.12691/wjac-1-1-2.

[23] J. Galceran, E. Companys, J. Puy, J. Cecilia, J.L. Garces, AGNES: a new electroanalytical technique for measuring free metal ion concentration, J. Electroanal. Chem. 566 (2004) 95–109. doi:10.1016/j.jelechem.2003.11.017.
[24] R.F. Domingos, C. Huidobro, E. Companys, J. Galceran, J. Puy, J.P. Pinheiro, Comparison of AGNES (absence of gradients and Nernstian equilibrium stripping) and SSCP (scanned stripping chronopotentiometry) for trace metal speciation analysis, J. Electroanal. Chem. 617 (2008) 141–148. doi:10.1016/j.jelechem.2008.02.002.
[25] L.S. Rocha, E. Companys, J. Galceran, H.M. Carapuça, J.P. Pinheiro, Evaluation of thin mercury film rotating disk electrode to perform absence of gradients and Nernstian equilibrium stripping (AGNES) measurements, Talanta. 80 (2010) 1881–1887. doi:10.1016/j.talanta.2009.10.038.
[26] M.H. Tehrani, E. Companys, A. Dago, J. Puy, J. Galceran, Free indium concentration determined with AGNES, Sci. Total Environ. 612 (2018) 269–275. doi:10.1016/j.scitotenv.2017.08.200.
[27] N. Serrano, J.M. Díaz -Cruz, C. Ari Environmental Analysis, Electroanalysis. 19 (2007) 2039–2049. doi:10.1002/elan.200703956.
[28] R.M. Town, H.P. van Leeuwen, Effects of adsorption in stripping chronopotentiometric metal speciation analysis, J. Electroanal. Chem. 523 (2002) 1–15. doi:10.1016/S0022-0728(02)00747-7.
[29] E. Companys, J. Galceran, J.P. Pinheiro, J. Puy, P. Salaün, A review on electrochemical methods for trace metal speciation in environmental media, Curr. Opin. Electrochem. 3 (2017) 144–162. doi:10.1016/j.coelec.2017.09.007.
[30] E.M. Thurman, R.L. Malcolm, Preparative isolation of aquatic humic substances, Environ. Sci. Technol. 15 (1981) 463–466. doi:10.1021/es00086a012.
[31] W.G. Botero, M. Pineau, N. Janot, R.F. Domingos, J. Mariano, L.S. Rocha, J.E. Groenenberg, M.F. Benedetti, J.P. Pinheiro, Isolation and purification treatments change the metal-binding properties of humic acids: effect of HF/HCl treatment, Environ. Chem. 14 (2018) 417–424. doi:10.1071/EN17129.
[32] S.C.C. Monterroso, H.M. Carapuca, J.E.J. Simao, A.C. Duarte, Optimisation of mercury film deposition on glassy carbon electrodes: evaluation of the combined effects of pH, thiocyanate ion and deposition potential, Anal. Chim. Acta. 503 (2004) 203–212. doi:10.1016/j.aca.2003.10.034.
[33] C. Parat, L. Authier, D. Aguilar, E. Companys, J. Puy, J. Galceran, M. Potin-Gautier, Direct determination of free metal concentration by implementing stripping chronopotentiometry as the second stage of AGNES, Analyst. 136 (2011) 4337–4343. doi:10.1039/C1AN15481H.
[34] J.P. Gustafsson, Visual MINTEQ version 3.0. KTH, Department of Land and Water Resources Engineering, Stockolm, Sweden, 2009. Available at http://vminteq.lwr.kth.se/, (n.d.).
[35] E.A. Biryuk, V.A. Nazarenko, R.V. Ravitskaya, Spectrophotometric determination of the hydrolysis constants of indium ions, Russian Journal of Inorganic Chemistry. 14 (1969) 503–506.
[36] W.W. Rudolph, D. Fischer, M.R. Tomney, C.C. Pye, Indium(III) hydration in aqueous solutions of perchlorate, nitrate and sulfate. Raman and infrared spectroscopic studies and ab-initio molecular orbital calculations of indium(III)–water clusters, Phys. Chem. Chem. Phys. 6 (2004) 5145–5155. doi:10.1039/B407419J.
[37] F. Vydra, K. Štulík, E. Juláková, Electrochemical stripping analysis., E. Horwood, Chichester, 1976.

[38] C. Huidobro, E. Companys, J. Puy, J. Galceran, J.P. Pinheiro, The use of microelectrodes with AGNES, J. Electroanal. Chem. 606 (2007) 134–140. doi:10.1016/j.jelechem.2007.06.001.
[39] E. Rotureau, Analysis of metal speciation dynamics in clay minerals dispersion by stripping chronopotentiometry techniques, Colloids Surf. Physicochem. Eng. Asp. 441 (2014) 291–297. doi:10.1016/j.colsurfa.2013.09.006.
[40] R.R. Nazmutdinov, T.T. Zinkicheva, G.A. Tsirlina, Z.V. Kuz'minova, Why does the hydrolysis of In(III) aquacomplexes make them electrochemically more active?, Electrochimica Acta. 50 (2005) 4888–4896. doi:10.1016/j.electacta.2005.02.091.
[41] J.M. Pingarron, R. Gallego-Andreu, P. Sanchez-Batanero, Potentiometric determination of stability constants of complexes formed by Indium(III) and different chelating agents, Bull. Soc. Chim. Fr. 3–4 (1984) 115–122.
[42] E. Vasca, D. Ferri, C. Manfredi, L. Torello, C. Fontanella, T. Caruso, S. Orrù, Complex formation equilibria in the binary Zn2+–oxalate and In3+–oxalate systems, Dalton Trans. 0 (2003) 2698–2703. doi:10.1039/B303202G.